

# E-Cadherin Tethered to Micropatterned Supported Lipid Bilayers as a Model for Cell Adhesion

Tomas D. Perez,<sup>†</sup> W. James Nelson,<sup>†</sup> Steven G. Boxer,<sup>‡</sup> and Lance Kam<sup>\*,‡</sup>

Department of Molecular and Cellular Physiology, Stanford University School of Medicine, Stanford, California 94305, and Department of Chemistry, Stanford University, Stanford, California 94305

Received August 19, 2005. In Final Form: September 22, 2005

Cell–cell adhesion is a dynamic process requiring recruitment, binding, and reorganization of signaling proteins in the plane of the plasma membrane. Here, we describe a new system for investigating how this lateral mobility influences cadherin-based cell signaling. This model is based on tethering of a GPI-modified E-cadherin protein (hEFG) to a supported lipid bilayer. In this report, membrane microfluidics and micropatterning techniques are used to adopt this tethered protein system for studies with the anchorage-dependent cells. As directly formed from proteoliposomes, hEFG exhibits a diffusion coefficient of  $0.6 \pm 0.3 \mu\text{m}^2/\text{s}$  and mobile fraction of 30–60%. Lateral structuring of the supported lipid bilayer is used to isolate mobile proteins from this mixed mobile/immobile population, and should be widely applicable to other proteins. MCF-7 cells seeded onto hEFG-containing bilayers recognize and cluster this protein, but do not exhibit cell spreading required for survival. By micropatterning small anchors into the supported lipid bilayer, we have achieved cell spreading across the bilayer surface and concurrent interaction with mobile hEFG protein. Together, these techniques will allow more detailed analysis of the cellular dynamics involved in cadherin-dependent adhesion events.

## Introduction

Cell–cell recognition is critical to development of multicellular tissues. Deregulation of such processes leads to alterations in cell association and migration, hallmarks of diseases such as cancer.<sup>1–3</sup> Intercellular engagement is accompanied by large-scale recruitment and rearrangement of adhesion protein complexes over distance scales on the order of tens of micrometers. To date, virtually all in vitro models examining the interaction of cells with purified cell–cell adhesion proteins fail to capture this lateral mobility, as the proteins are immobilized onto a culture surface. A notable system that captures this mobility is the supported lipid bilayer model, which consists of a lipid bilayer in close association with an appropriate support such as glass.<sup>4,5</sup> Specifically, proteins that are tethered to the supported lipid bilayer exhibit lateral mobility along the plane of the bilayer.<sup>6</sup> This approach has found great success in the study of the immunological synapse;<sup>7–9</sup> T-cells recognize and reorganize proteins that are tethered to lipid bilayers via a glycosylphosphatidyl inositol (GPI) moiety, enhancing cellular response as compared to that from immobilized proteins. Adaptation of the supported lipid bilayer model for use with other cell types, and anchorage dependent

cells in particular, has much promise in revealing the effect of lateral mobility in cell–cell communication.

We report two advancements on the basic supported lipid bilayer model that will facilitate studies involving anchorage dependent cells. This model focuses on epithelial cell recognition of E-cadherin, a member of the cadherin family of transmembrane cell–cell adhesion proteins<sup>10,11</sup> involved in initiation of epithelial cell–cell contacts and subsequent assembly of intracellular adhesion complexes that control paracellular diffusion (tight junctions) and maintain the structural continuum of the epithelium (desmosomes). These functions are thought to involve the formation of multiple *cis*-dimers of E-cadherin on each cell surface which subsequently interact as *trans*-oligomers between opposing cell surfaces.<sup>12–15</sup> E-cadherin, cytoskeletal actin, and other intracellular proteins exhibit complex changes dramatically during initiation and maturation of cell–cell contacts.<sup>16,17</sup> To capture these spatial dynamics in a controllable, in vitro system, we tethered the extracellular domain of human E-cadherin to supported lipid bilayers via a GPI moiety, as inspired by studies into the immunological synapse. However, this basic configuration faces several limitations in regards to use with epithelial cells or other anchorage dependent cells; this report addresses two fundamental challenges. First, no GPI-tethering method described to date intrinsically ensures that the proteins are laterally mobile. While the percentage of total incorporated proteins that are laterally mobile, or mobile fraction, has been reported to

\* Corresponding author. Current address: Department of Biomedical Engineering, Columbia University, New York, NY 10027.

<sup>†</sup> Department of Molecular and Cellular Physiology, Stanford University School of Medicine.

<sup>‡</sup> Department of Chemistry, Stanford University.

(1) Gumbiner, B. M. *Cell* **1996**, *84*, 345–357.  
 (2) Yap, A. S. *Cancer Invest.* **1998**, *16*, 252–261.  
 (3) Takeichi, M. *Curr. Opin. Cell Biol.* **1995**, *7*, 619–627.  
 (4) Groves, J. T.; Boxer, S. G. *Acc. Chem. Res.* **2002**, *35*, 149–157.  
 (5) Sackmann, E. *Science* **1996**, *271*, 43–48.  
 (6) Groves, J. T.; Wulfing, C.; Boxer, S. G. *Biophys. J.* **1996**, *71*, 2716–2723.  
 (7) Chan, P. Y.; Lawrence, M. B.; Dustin, M. L.; Ferguson, L. M.; Golan, D. E.; Springer, T. A. *J. Cell Biol.* **1991**, *115*, 245–255.  
 (8) Grakoui, A.; Bromley, S. K.; Sumen, C.; Davis, M. M.; Shaw, A. S.; Allen, P. M.; Dustin, M. L. *Science* **1999**, *285*, 221–227.  
 (9) Groves, J. T.; Dustin, M. L. *J. Immunol. Methods* **2003**, *278*, 19–32.

(10) Kemler, R. *Semin. Cell Biol.* **1992**, *3*, 149–155.  
 (11) Frank, M.; Kemler, R. *Curr. Opin. Cell Biol.* **2002**, *14*, 557–62.  
 (12) Yap, A. S.; Niessen, C. M.; Gumbiner, B. M. *J. Cell Biol.* **1998**, *141*, 779–789.  
 (13) Yap, A. S.; Brieher, W. M.; Pruschy, M.; Gumbiner, B. M. *Curr. Biol.* **1997**, *7*, 308–315.  
 (14) Brieher, W. M.; Yap, A. S.; Gumbiner, B. M. *J. Cell Biol.* **1996**, *135*, 487–496.  
 (15) Pokutta, S.; Herrenknecht, K.; Kemler, R.; Engel, J. *Eur. J. Biochem.* **1994**, *223*, 1019–1026.  
 (16) Adams, C. L.; Chen, Y. T.; Smith, S. J.; Nelson, W. J. *J. Cell Biol.* **1998**, *142*, 1105–1119.  
 (17) Ehrlich, J. S.; Hansen, M. D.; Nelson, W. J. *Dev. Cell* **2002**, *3*, 259–270.

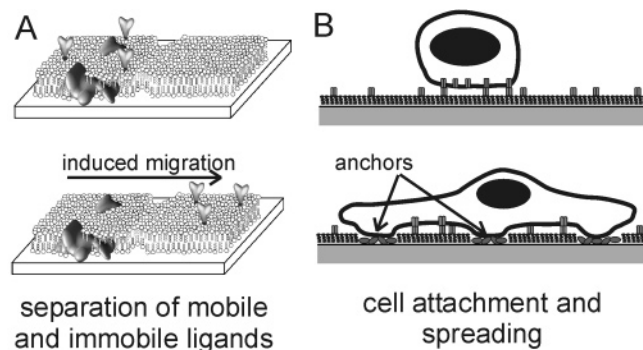


**Figure 1.** Schematic descriptions of the two methods demonstrated in this report. (A) Mobile, membrane-tethered proteins are separated from their immobile counterparts, which invariably result from the bilayer formation process, by creating an adjacent, defined region of protein-free lipid bilayer. Mobile proteins migrate to the region free of immobile proteins. (B) Substrate containing only mobile, tethered ligands cannot support cell spreading. Micropatterning of cell adhesive anchors into this system provides for cell spreading while maintaining fluidity of the supported lipid bilayer.

be as high as 90%, a significant percentage of the proteins are immobile, confounding interpretation of cell recognition data. Second, given the viscous properties of typical cell membranes, membrane-tethered ligands cannot significantly resist the piconewton forces generated by cells. Consequentially, the basic supported lipid bilayer model cannot support cell spreading, an activity required for survival of anchorage-dependent cells.<sup>18,19</sup>

The approaches presented here are based on micropatterning and lateral structuring of supported lipid bilayers,<sup>4,20–24</sup> concepts originally developed to locally direct lipid membrane diffusion which have further evolved to include the incorporation of complementary biological function.<sup>24</sup> As illustrated in Figure 1A, the issue of immobile fraction is addressed by creating two adjacent and connected regions of lipid bilayer; the first contains both mobile and immobile counterparts of the target protein, while the second is a bilayer containing no tethered proteins. Taking advantage of simple diffusion or induced migration, mobile (but not immobile) targets are moved to the latter region, yielding a population of only mobile targets. As developed for cell adhesion assays, the region containing this population can in concept be several hundred micrometers in dimension. A different application of bilayer patterning is used to address the issue of cell adhesion onto a surface of mobile ligands, as illustrated in Figure 1B. Namely, an array of cell-adhesive, immobilized anchors are patterned into the supported lipid bilayer. The dimensions of this array are small compared to a cell, allowing cells to spread across multiple anchors while exposing a large region of the cells to the supported lipid bilayer and tethered proteins. Implemented either together or separately, these methods significantly advance model systems for investigating the role of protein mobility in modulating cell–cell communication.

## Materials and Methods

**Protein and Proteoliposome Production.** GPI-anchored, human E-cadherin/Fc (hEFG, Figure 2A) was produced using standard cloning and protein production techniques. The open

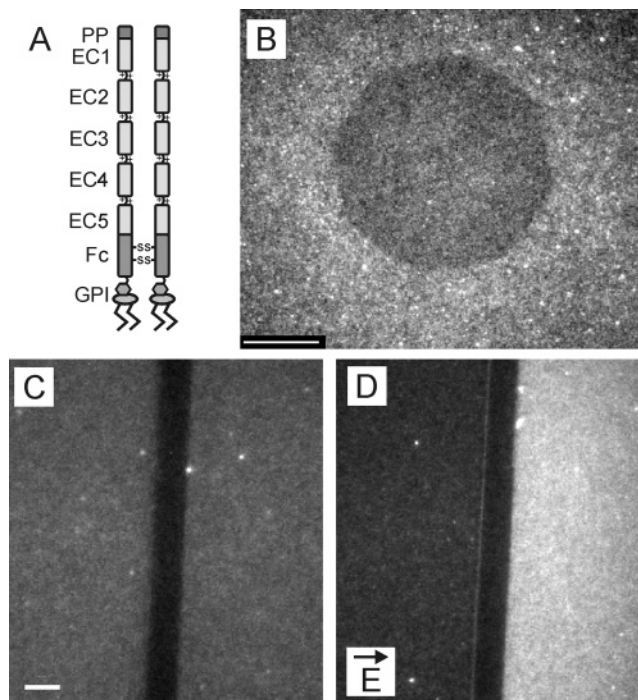


**Figure 2.** (A) Schematic of a dimer of hEFG protein, each of which consists of the extracellular domain of human E-cadherin (EC1–EC5), an Fc domain, and a GPI tether. PP = pre-peptide sequence, which is normally removed from E-cadherin after translation. (B) Supported bilayer of egg PC containing Cy5-labeled, GPI-tethered hEFG, 30 min after photobleaching of the octagonal region in the middle of this frame. The white scale bar (lower left) = 25  $\mu\text{m}$ . (C) A Cy5-hEFG bilayer containing a diffusion barrier (vertical dark line) created by scratching the substrate, removing bilayer and protein from that region. (D) Migration and accumulation of hEFG against the scratch barrier under influence of an applied 23 V/cm field. Panels C and D are shown at identical magnification; scale bar in panel B = 25  $\mu\text{m}$ .

reading frame encoding this protein contains the extracellular domain of E-cadherin (complete with upstream signal sequence, a gift from Dr. Jonathan Higgins, Harvard Medical School), appended with the hinge and constant region of human IgG1<sup>25</sup> and the GPI signal sequence of human placental alkaline phosphatase (generously provided by Mark Davis, Stanford University<sup>26</sup>). This sequence was inserted into a pcDNA3.1A(+) vector and then transfected into HEK 293 cells which were selected using 400  $\mu\text{g}/\text{mL}$  G418. For a production batch, ten (10) 150 mm tissue culture dishes of cells were grown to confluency. Cells were washed with cold (4  $^{\circ}\text{C}$ ) phosphate buffered saline (PBS, 10 mM phosphate, pH 7.4, 135 mM NaCl, 5 mM KCl), and then hEFG protein was extracted from the cells using 1% *n*-octyl- $\beta$ -D-glucopyranoside (OG) in PBS containing EDTA-free Complete Protease Inhibitor cocktail tablets (Roche) and purified using a Protein A Sepharose (Amersham) column. Protein was dialyzed against storage buffer (SB, 10 mM HEPES pH 7.4, 154 mM NaCl, 7.2 mM KCl, 1% OG) and then flash frozen and stored at  $-80$   $^{\circ}\text{C}$  at 200  $\mu\text{g}/\text{mL}$  (as determined using the BCA assay; Pierce, Rockford, IL), 25  $\mu\text{L}$  per aliquot. SDS–PAGE/Western blot analyses on purified hEFG protein were performed using either the antibody HECD-1 (Calbiochem, La Jolla, CA), with an HRP-conjugated secondary antibody to HECD-1, or an HRP-conjugated anti-human Fc IgG antibody; an ECL kit was used to detect the

(22) Kam, L.; Boxer, S. G. *J. Am. Chem. Soc.* **2000**, *122*, 12901–12902.

(23) Kam, L.; Boxer, S. G. *Langmuir* **2003**, *19*, 1624–1631.

(24) Kam, L.; Boxer, S. G. *J. Biomed. Mater. Res.* **2001**, *55*, 487–495.

(18) McBeath, R.; Pirone, D. M.; Nelson, C. M.; Bhadriraju, K.; Chen, C. S. *Dev. Cell* **2004**, *6*, 483–495.

(19) Chen, C. S.; Mrksich, M.; Huang, S.; Whitesides, G. M.; Ingber, D. E. *Science* **1997**, *276*, 1425–1428.

(20) Boxer, S. G. *Curr. Opin. Chem. Biol.* **2000**, *4*, 704–9.

(21) Groves, J. T.; Ulman, N.; Boxer, S. G. *Science* **1997**, *275*, 651–653.

(25) Taraszka, K. S.; Higgins, J. M. G.; Tan, K.; Mandelbrot, D. A.; Wang, J.-h.; Brenner, M. B. *J. Exp. Med.* **2000**, *191*, 1555–1567.

(26) Whitehorn, E. A.; Tate, E.; Yanofsky, S. D.; Kochersperger, L.; Davis, A.; Mortensen, R. B.; Yonkovich, S.; Bell, K.; Dower, W. J.; Barrett, R. W. *Biotechnology (N.Y.)* **1995**, *13*, 1215–1219.



HRP signal. Both antibodies revealed only two protein bands. The major band (~120 kDa) corresponds to full-length hEFG, while a minor band (~130 kDa) likely corresponds to uncleaved hEFG precursors containing an initial pre-peptide sequence (data not shown). Bead aggregation assays demonstrated that hEFG retained calcium-dependent adhesive activity (data not shown). These assays were carried out by mixing 5 mL of Protein A-modified magnetic beads ( $2 \times 10^9$  beads/mL, 3 mm diameter DynaBeads, Dynal, Brown Deer, WI) with 4  $\mu$ g of hEFG. Beads were rinsed and resuspended in buffer with either 4 mM  $\text{CaCl}_2$  or 10 mM EDTA. Large clusters (>10 beads) of hEFG-bearing beads were formed in the presence of 3.5 mM  $\text{Ca}^{2+}$  but not in EDTA-containing media. This clustering was not observed in the absence of hEFG protein. For experiments using fluorescently labeled hEFG, protein was labeled with Cy5 NHS ester stock (Amersham) at a 15:1 dye: protein molar ratio in SB, conditions chosen to promote N-terminal labeling of the protein. The reaction was then either dialyzed overnight against SB in a 10 kDa MWCO minidialysis unit (Pierce) before incorporating into proteoliposomes or incorporated immediately following labeling; both methods resulted in protein-specific labeling, which was verified by carrying out labeling and proteoliposome preparation steps without hEFG protein.

Stock solutions of small unilamellar vesicles of egg phosphatidylcholine (egg PC) (Avanti Polar Lipids, Alabaster, AL) were prepared by extrusion through 50 nm pore membranes (extruder and membranes from Avanti) at 5 mg/mL in vesicle buffer 1 (VB1; 10 mM HEPES, 140 mM NaCl, 5 mM KCl, pH 8.5 at 4°C). For visualization and demonstration purposes, vesicles were supplemented with 0.5 mol % of a neutral, NBD-labeled phospholipid (NBD-PC, 1-acyl-2-[12-[(7-nitro-2-1,3-benzoxadiazol-4-yl)amino]dodecanoyl]-sn-glycero-3-phosphocholine; Avanti). For each batch of proteoliposomes, a 100  $\mu$ L aliquot of vesicles was mixed with 25  $\mu$ L of 5% OG in VB1 and vortexed briefly. This lipid solution was mixed with 25  $\mu$ L (5  $\mu$ g) of hEFG protein (either unlabeled or labeled with Cy5), incubated at room temperature for 1 h, and then dialyzed for 2 days at 4°C against  $2 \times 1$  L volumes of VB1; the dialysis buffer was changed once after the first day. The calculated lipid: protein ratio of  $3.1 \times 10^4$  was modified in certain experiments (indicated in the Results) by changing the concentration of protein. The resultant proteoliposome solutions were stored at 4°C and used within 1 week.

**Substrate Preparation.** Glass coverslips were cleaned by immersion into Linbro 7X detergent (ICN Biomedicals, Inc., Aurora, OH) diluted 1:3 (v/v) in deionized water, then baked at 450°C for 4 h. Microcontact printing using Sylgard 184 stamps was performed as previously described.<sup>23,24,27</sup> For all stamping steps, fibronectin was labeled with monoamine-reactive Cy3.5 (Amersham) following the manufacturer's instructions and then mixed 1:3 with unlabeled protein for a total concentration of 100  $\mu$ g/mL.

Lipid bilayers were formed on surfaces inside a silicone perfusion gasket (CoverWell, 9 mm diameter, 0.5 mm thick, Molecular Probes, Eugene, OR). The chamber was filled with proteoliposome solution mixed 2:1 with fusion buffer (FB; 20 mM Tris, 140 mM NaCl, 5 mM KCl, pH 8.6) for at least 10 min and then rinsed extensively with PBS. Electrophoresis was carried out on these surfaces as previously described.<sup>28</sup> The fraction of total hEFG protein that was laterally mobile, or mobile fraction, was measured by fluorescence recovery after photobleaching (FRAP). A large (50–100  $\mu$ m) octagonal region of an unpatterned bilayer containing Cy5-labeled hEFG was photobleached. The mobile fraction of hEFG was calculated by comparing the average fluorescence intensity within this spot before and 30 min after photobleaching. The average intensity measured immediately after a subsequent, extended photobleach period was used to determine background intensity and subtracted from values used for this calculation. The diffusion coefficient for hEFG was calculated by following the time evolution of a nonuniform distribution of Cy5-labeled hEFG by electrophoresis,<sup>29</sup> as detailed in the Results and Discussion.

As an alternative configuration, a converging channel apparatus described previously<sup>22,23</sup> was used to control the compositional distribution of a lipid bilayer formed from two different types of vesicles. Bilayers were formed in these channels as previously described.<sup>22,23</sup>

**Cell Culture and Adhesion Assays.** MCF-7 cells (ATCC) were maintained in DMEM + 10% FBS under standard cell culture conditions and used between passages 9 and 18 for these experiments. Cells at 50% confluency were split 1:4 the day before use in each experiment. For visualization purposes, cells were loaded with CellTracker Green (Molecular Probes) at 40  $\mu$ g/mL in DMEM + 10% FBS for 2 h. Alternatively, cells were transfected with EYFP-Mem, a membrane-targeted, palmitoylated variant of YFP (EYFP-Mem, Clontech), using Lipofectamine 2000 (LifeTechnologies). While this second method resulted in different levels of YFP expression by individual cells within a population, better definition of spread cells was achieved due to selective localization to cell membranes.

For assays of cell attachment and adhesion, supported lipid bilayers, in a gasket, were blocked with 1 mg/mL BSA (Sigma) in FB for 30 min. The chambers were then rinsed with DMEM + 5% FBS. MCF-7 cells were trypsinized (Gibco; 0.5% Trypsin; 5.3 mM EDTA-4Na, diluted 1:9 into HBS buffer (10 mM HEPES, 140 mM NaCl, 5 mM KCl, pH 7.4)) at room temperature until cells were just loosely attached, then seeded onto the surfaces at a concentration of  $5 \times 10^4$  cells/mL in DMEM + 5% FBS that had been equilibrated in a cell culture incubator for 2 h. At specified times, chambers were rinsed twice with HBS and the samples fixed using 4% paraformaldehyde; throughout this process the chamber was never empty and the bilayer was not exposed to air.

All images were collected using a Nikon Eclipse inverted microscope equipped with a mercury arc lamp, appropriate filter sets, an intensified PentaMax 512 HQ, and a Cascade 650 (both cameras from Roper Scientific, Trenton, NJ).

## Results and Discussion

This report centers on the fusion protein hEFG, which is based on the extracellular domain of human E-cadherin appended with the Fc domain of human IgG; this chimera strategy has been used extensively in the study of cadherin function<sup>13,30–32</sup>. The hEFG protein additionally contains a GPI-moiety (Figure 2A), which has been used to tether other proteins to a supported lipid bilayer, specifically in the context of T cell interaction with antigen presenting cells.<sup>6–8</sup> With respect to obtaining laterally mobile biomolecules, the hEFG protein presented several obstacles compared to GPI-tethered proteins in other reports, inspiring a technique for purifying mobile proteins from a mixed population. This section begins with a focus on membrane-tethered hEFG and then demonstrates the use of the two strategies presented in Figure 1 to create advanced surfaces for use in studies of cell signaling.

**Membrane-Tethered hEFG.** Supported lipid bilayers containing tethered hEFG molecules, formed by fusion of Cy5-labeled hEFG/egg PC proteoliposomes onto borosilicate glass, appeared uniform over large distance scales (hundreds of micrometers to millimeters). At higher magnification, two populations of proteins were observed. These are illustrated in Figure 2B, which shows a supported bilayer containing Cy5-labeled hEFG imaged 30 min after photobleaching of a ~70  $\mu$ m octagonal spot in the field of view. The signal inside the spot represents recovery after the initial photobleach; the grayscale level in this figure was adjusted such that in a paired image collected immediately after photobleaching, the center of the spot was completely black. Outside of the photobleach region was an additional population of bright spots that

(27) Kung, L. A.; Kam, L.; Hovis, J. S.; Boxer, S. G. *Langmuir* **2000**, *16*, 6773–6776.

(28) Groves, J. T.; Boxer, S. G. *Biophys. J.* **1995**, *69*, 1972–1975.

(29) Tsay, T. T.; Jacobson, K. A. *Biophys. J.* **1991**, *60*, 360–368.

(30) Niessen, C. M.; Gumbiner, B. M. *J. Cell Biol.* **2002**, *156*, 389–399.

(31) Chappuis-Flament, S.; Wong, E.; Hicks, L. D.; Kay, C. M.; Gumbiner, B. M. *J. Cell Biol.* **2001**, *154*, 231–243.

(32) Perret, E.; Benoliel, A. M.; Nassoy, P.; Pierres, A.; Delmas, V.; Thiery, J. P.; Bongrand, P.; Feracci, H. *Embo. J.* **2002**, *21*, 2537–2546.

did not change position between successive images, indicative of a population of immobile proteins. On the basis of quantitative comparison of the Cy5 signal before and 30 min after photobleaching, we routinely obtained mobile fractions of hEFG of 30–60%.

The diffusion coefficient for hEFG was calculated by following the time evolution of freely diffusing Cy5-labeled hEFG. However, low fluorescence intensity and photobleaching of the Cy5-hEFG signal severely impeded the collection of these time series in the FRAP experiments used to determine mobile fraction. Instead, electrophoresis was first used to accumulate hEFG protein against a diffusion barrier produced by scratching the sample surface (Figure 2, parts C and D). As demonstrated previously, this procedure yields large increases in local concentration of tethered proteins near the barriers;<sup>6</sup> here, the higher concentrations were used to offset the effects of photobleaching. A series of images taken at regular intervals were collected from these surfaces after removal of the electric field, and intensity profiles perpendicular to the barrier were generated from these images. Intensity profiles collected over at least 8 min were used to calculate a diffusion coefficient for hEFG.<sup>29</sup> On the basis of this analysis, hEFG protein tethered to supported lipid bilayers of egg PC exhibits Brownian diffusion with a diffusion coefficient of  $0.6 \pm 0.3 \mu\text{m}^2/\text{s}$  ( $n = 4$ ).

Membrane-tethered hEFG exhibited diffusive properties that were very different than other GPI-tethered proteins such as I-E<sup>k</sup>, B7-2, and CD48 reported earlier by Groves et al.<sup>6</sup> First, during the electrophoresis process, hEFG migrated toward the anode (Figure 2D), opposite in direction to the GPI-tethered proteins in the Groves report, which migrated toward the cathode. A model of membrane protein electrophoresis by McLaughlin and Poo<sup>33</sup> relates migration direction to a balance between biomolecular charge and coupling to electroosmotic flow effected by soluble countercharges near the membrane; in support of the model, both cathodic and anodic migration of cell surface proteins are demonstrated in that report. On the basis of a qualitative interpretation of this model and the fact that the current study uses supported lipid bilayers of similar lipid composition to that in the Groves report, it is postulated that hEFG is more negatively charged than the GPI-anchored proteins in that study.

A second difference is that the maximum areal density of mobile hEFG protein that could be formed directly by fusion of the proteoliposomes to glass is low. Mobile fraction of hEFG was related to the protein: lipid ratio, and the ratio of 1:30 000 used throughout this report provided the maximum mobile fraction of 30–60%. Doubling the amount of hEFG protein relative to lipids resulted in a nearly complete loss of mobile proteins, while doubling the amount of lipid relative to protein, though not significantly affecting the mobile fraction, reduced the areal concentration of protein without increasing the mobile fraction (data not shown). Assuming complete incorporation of proteins and lipids into proteoliposomes and subsequently into the supported lipid bilayers, the optimized protein: lipid ratio of 1:30,000, which provided the highest mobile fraction of 30–60%, corresponds to a surface density of hEFG dimers of  $\sim 55$  molecules/ $\mu\text{m}^2$  of lipid bilayer. This concentration is on the order of that estimated on noninteracting surfaces of cells,<sup>34</sup> but is orders of magnitude lower than that used in experiments involving cadherins immobilized on beads;<sup>35</sup> the ability to create higher concentrations of mobile proteins to bridge these classes of studies is clear. Moreover, this concentration compares to densities of up to 200 molecules/ $\mu\text{m}^2$  reported for a GPI-tethered form of ICAM1<sup>8</sup> and  $1 \times 10^3$

molecules/ $\mu\text{m}^2$  for the proteins reported by Groves.<sup>6</sup> Since electrophoresis successfully yielded a concentrated population of hEFG on the lipid bilayer (Figure 2D), it is concluded that this limitation in areal density of hEFG observed in directly formed bilayers is not an intrinsic property of the protein, but rather attributed to the bilayer formation process.

The idea that both the limitation on areal density and the formation of an immobile fraction result from the bilayer formation process was further investigated. The presence of immobile proteins was not reduced when the proteoliposomes were first purified using an Optiprep gradient (initial uniform density of 1.15 g/mL, centrifugation at 200 000 RCF for 2 h, which caused the proteoliposomes to float), suggesting that the immobile fraction does not come from proteins that are not incorporated into the proteoliposomes. The pH of buffers used during proteoliposome preparation and fusion were varied from 7 to 9.0 by 0.5 unit increments. For both buffers, pH 8.5 yielded the maximum mobile fractions; higher and lower pH values resulted in lower mobile fractions (data not shown).

Last, the protein:lipid ratio of 1:30 000 yields roughly 1 hEFG molecule per 50 nm vesicle. It is entirely possible that half of the proteins, which are assumed to incorporate onto the outside of the vesicles,<sup>36</sup> would encounter the glass surface and become immobilized on the glass before an underlying supported bilayer can form. Labeling of hEFG-containing bilayers using an antibody directed toward the Fc domain revealed both mobile and immobile populations (data not shown) suggesting that the immobile proteins would be accessible to cells. Since the hEFG protein appears to be more negatively charged than GPI-tethered I-E<sup>k</sup>, CD48, and B7-2 (as described above) it might be reasonable to expect that hEFG would be repelled from the surface more than these proteins or indeed the lipids. This effect would serve to increase or at least not decrease the mobile fraction compared to the other proteins, which is not the observed result. We also observed that a canine version of hEFG, structurally similar to hEFG but composed of the extracellular domain of canine E-cadherin and produced ancillary to this report, is almost completely immobile, even after extensive reoptimization of the vesicle fusion conditions. We conclude that while attention to the vesicle fusion process has yielded an optimized preparation of mobile hEFG molecules for this study, the factors governing the generation and extent of the immobile fraction remain unclear and dependent on the specific protein being tethered.

**Mobility-Based Purification of hEFG.** The low yield of mobile proteins obtained with hEFG inspired the use of membrane microfluidics,<sup>23</sup> to obtain purified populations of mobile ligands. The configuration illustrated in Figure 1A was created using a converging microfluidic channel (Figure 3A) which exposed a micropatterned surface to two vesicle solutions. This configuration is shown again schematically in the bottom panel of Figure 3A, and an implementation of this system in Figure 3B, consisting of a 1 mm  $\times$  500  $\mu\text{m}$  corral defined by barriers of fibronectin encompassing the two connected bilayer regions; for these experiments, fibronectin was chosen for its effectiveness as a barrier. Figure 3C shows this same region after a 120

(33) McLaughlin, S.; Poo, M. M. *Biophys. J.* **1981**, *34*, 85–93.

(34) Duguay, D.; Foty, R. A.; Steinberg, M. S. *Dev. Biol.* **2003**, *253*, 309–323.

(35) Lambert, M.; Padilla, F.; Mege, R. M. *J. Cell. Sci.* **2000**, *113* (Part 12), 2207–2219.

(36) Salafsky, J.; Groves, J. T.; Boxer, S. G. *Biochemistry* **1996**, *35*, 14773–14781.



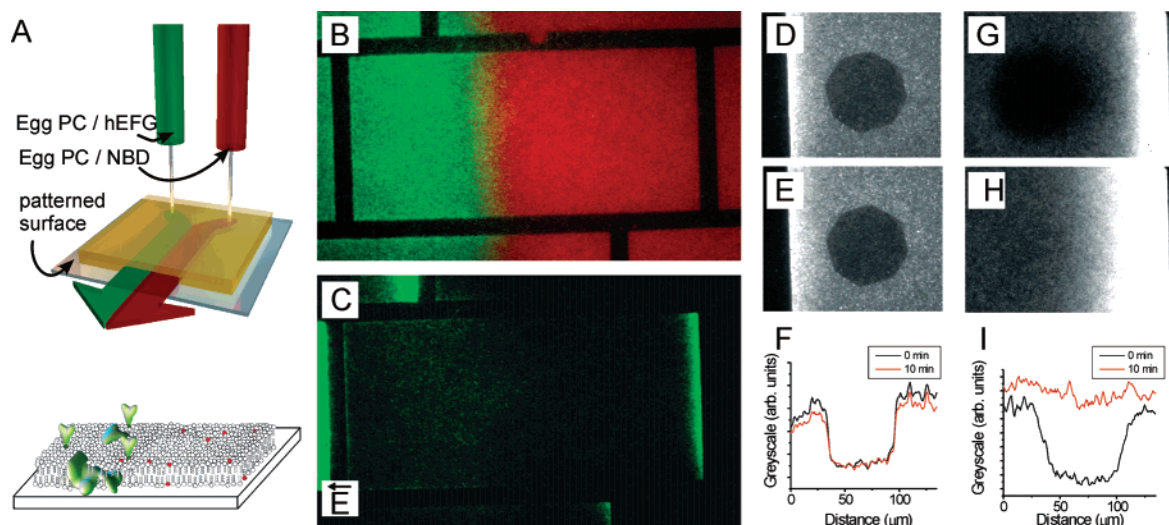


**Figure 3.** (A) Schematic diagrams of the converging flow system used to create laterally complex supported lipid bilayers. (B) A  $1 \text{ mm} \times 500 \mu\text{m}$  corralled membrane. The left side contains a mixed population of mobile and immobile hEFG molecules (green) incorporated into an egg PC bilayer. The right side contains a bilayer doped with a small amount of fluorescently labeled NBD-lipid (red). (C) Migration of mobile hEFG proteins to the right side of the corral shown in panel B. The NBD-lipid signal is omitted from this frame for clarity. (D–I) Recovery of  $70 \mu\text{m}$ -wide photobleach spots, located near the left (panels D–F) or right (panels G–I) edge of the corral. Panels D and G were taken immediately after photobleaching, while panels E and H were taken 10 min later. The line traces in panels F and I were derived from profiles taken vertically across the center of each photobleached spot.

min application of an electric field of  $20 \text{ V/cm}$  tangential to this surface. Mobile hEFG migrated from the left side of the corral to the right; the red signal, associated with the small amount of uncharged NBD-labeled lipid used to visualize the protein-free bilayer region, did not change significantly over this time and is omitted from this panel for clarity. Fluorescence recovery after photobleaching experiments (Figure 3D–I), carried out by photobleaching a  $70 \mu\text{m}$  diameter spot of the hEFG-associated Cy5 signal and observing recovery of the resultant fluorescence profile over 10 min, indicate that the hEFG molecules on the left side of the corral are completely immobile while no immobile fraction was detected on the right side of the corral. It is emphasized that completely mobile populations are obtained not by optimizing the bilayer formation conditions but by manipulating the membrane and tethered proteins after bilayer formation. As stated above, the hEFG protein did not yield high mobile fractions, even with extensive optimization of bilayer formation conditions. Isolation of mobile proteins on the basis of mobility is thus a powerful strategy for handling proteins that intrinsically do not yield high mobile fractions. Furthermore, this approach should be widely applicable to other proteins, allowing the production of completely mobile populations without extensive reoptimization of bilayer formation conditions.

A mechanism for preventing diffusion of mobile hEFG away from the right-side barrier after removal of the electric field would be clearly useful for maintaining a high concentration of these targets. On the surfaces illustrated in Figure 3, this capability could also be used to prevent remixing of the mobile proteins back into the regions containing immobile proteins. We suggest that mechanical disruption of the surface (i.e., scratching the supported bilayer<sup>37</sup>) or further use of microfluidics to selectively remove portions of the bilayer (using a detergent solution, for example<sup>23</sup>) would achieve this capability, but to date, implementation of such methods with the required spatial accuracy has been elusive.

#### Cell Recognition of Membrane-Tethered hEFG.

The ability of epithelial cells to recognize and interact with hEFG was examined by seeding MCF-7 cells onto hEFG-containing supported lipid bilayers. At 6 h after

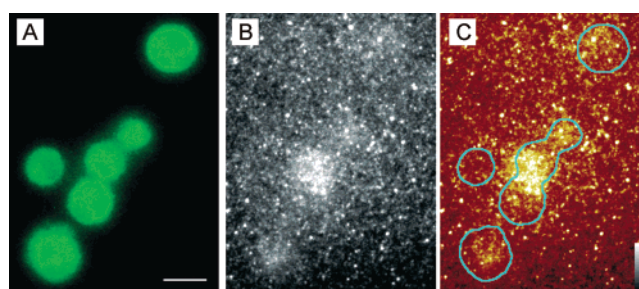


**Figure 4.** 6 h interaction of MCF-7 cells and a bilayer containing hEFG. (A) Cells (green) were rounded in morphology. (B) Cy5-labeled hEFG, which was observed only in the plane of the lipid bilayer. (C) Outline of attached cells (light blue lines) overlaid onto a color-mapped version of the grayscale image in part B, demonstrating correlation of hEFG clusters and cell attachment; the color map is indicated in the lower right corner of this panel. The scale bar in panel A =  $10 \mu\text{m}$ .

seeding, cells exhibited a rounded morphology indicative of loosely attached cells (Figure 4, parts A and C). For visualization purposes, the cells were loaded with CellTracker Green while hEFG protein was labeled with Cy5. About 30% of these cells (17 out of 52 observed cells), such as the cell in the center of Figure 4, parts A and C, were associated with localized regions of higher hEFG concentration measuring several micrometers in size and in the plane of the lipid bilayer (Figure 4, parts B and C). These clusters of hEFG protein indicate recognition and binding of laterally mobile hEFG protein by the MCF-7 cells. The presence of cells under which no clustering was observed (such as the upper right cell in Figure 4, parts A and C), and the absence of clusters not associated with cells suggest that this interaction is hEFG specific and not simply the result of other processes, such as passive trapping of mobile molecules between the cell and membrane. We suggest that the cells under which no clustering is observed most likely have not recovered from the dissociation and seeding steps. Quantification of the fluorescence signal associated with these clusters indicates

(37) Cremer, P. S.; Groves, J. T.; Kung, L. A.; Boxer, S. G. *Langmuir* 1999, 15, 3893–3896.

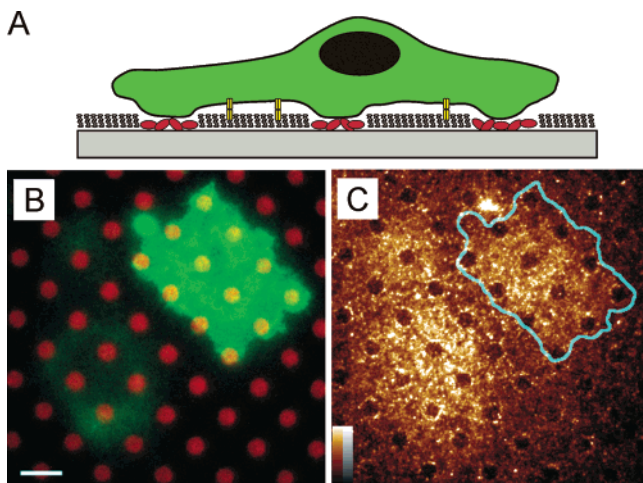


**Figure 5.** (A) Schematic of cell adhesion to the micropatterned surface, color coded to correspond to the other panels in this figure. (B) 4 h adhesion of MCF-7 cells (green) onto a hEFG/egg PC bilayer surface micropatterned with an array of 5  $\mu\text{m}$  diameter fibronectin dots (red). MCF-7 cells were transfected with EYFP-Mem, yielding a mixed population of cells expressing different levels of this protein. This panel contains three cells, which are all detectable at long exposure; the cell visible in the upper right of this lower exposure image expressed the highest level of EYFP. (C) Cy5-hEFG distribution in the same field of view as panel B. Color map is shown in the lower left corner of this panel. The outline of the bright cell shown in Panel B is overlaid in light blue. Scale bar = 10  $\mu\text{m}$ .

an increase of 15–35% in fluorescence intensity, averaged over the total projected cell area, compared to regions of the bilayer not interacting with cells. Assuming a mobile fraction of hEFG of 30–60% in these bilayers, this corresponds to a 1.2–2.3-fold increase in average fluorescence intensity associated with mobile protein; the immobile population contributes a constant component to the intensity measured both under and away from the cell, giving the appearance of a lower relative increase in concentration of mobile protein. Furthermore, these numbers were calculated using the raw, nonbaselined values reported by the digital camera. As the true background fluorescence of the supported lipid bilayer (which would be greater than zero and, in these studies, was about 20% of the total signal) would also appear as a constant numerical component of each signal, the relative increase in signal associated with the mobile population of hEFG would be higher.

While cells were able to recognize and cluster the hEFG protein tethered to an unpatterned supported lipid bilayer, Figure 4 illustrates the fundamental challenge in the interaction of anchorage dependent cells with mobile ligands; cells cannot spread across these surfaces. The observation that only 30% of cells actually clustered the hEFG protein, potentially indicative of nonviable cells as noted above, further suggests that the unpatterned, hEFG bilayer model is not an effective model of cell–protein interaction. The ability of micropatterning to address both of these behaviors is demonstrated in the next section.

**Cell Spreading on Micropatterned hEFG Surfaces.** The approach of using small anchors to allow cell spreading, while facilitating cell interaction with mobile ligands is demonstrated in Figure 5. The schematic of this interaction is repeated in Figure 5A, which reflects the color coding of components in the other panels. Parts B and C on Figure 5 illustrate 4 h adhesion of MCF-7 cells (green) on a surface patterned with an array of 5  $\mu\text{m}$  diameter anchors of fibronectin (red) spaced 10  $\mu\text{m}$  apart; if the anchors are spaced at sufficiently fine distances

and of appropriate dimension,<sup>24</sup> cells can attach to multiple anchors, spreading across a bilayer surface. For these experiments, MCF-7 cells were transfected with a membrane-associated version of EYFP (EYFP-Mem), allowing better visualization of the cell morphology compared to cell-filling labels such as that shown in Figure 4. However, transient transfection resulted in a mixed population of cells expressing different levels of EYFP-Mem; the field of view shown in Figure 5, parts B and C, includes three cells, all visible at high camera sensitivity and long exposure, but only one is expressing an appreciable level of EYFP-Mem and is outlined in Figure 5C. In a long exposure image, which details the morphology of the two dim cells, all other features are highly saturated; for this reason, the long exposure image is omitted. In addition to spreading across the surface via the micropatterned anchors, cells interact with ligands presented on the supported lipid bilayer, evidenced by the clustering of hEFG protein illustrated in Figure 5C. It is further noted that with few exceptions, cells that spread across multiple anchors clustered the hEFG protein, suggesting that these cells are viable and an appropriate model of cell–protein interaction. Over the entire projected cell area, the increase in hEFG-associated fluorescence was typically 30%, corresponding to a 1.5–2-fold-increase in mobile protein, subject to the same analysis described for cells on unpatterned surfaces. The concept of using arrays of subcellular, adhesive regions to allow cell spreading across a surface is well established,<sup>19,24,38</sup> but the use of this concept to promote interaction of cells not with the features themselves but with targets associated with the intervening regions, and specifically with membrane tethered proteins, is a new and novel combination of several underlying methodologies.

## Conclusion

Cell–cell contacts are highly dynamic interfaces; experimental models that provide control over the distribution and mobility of purified proteins presented to cells will greatly extend understanding of the intracellular signaling cascades influenced by these long-range effects. In the context of E-cadherin-based cell signaling, we have demonstrated a model of adherent cell interaction with purified proteins that will facilitate these studies, such as the role of various regulatory proteins (e.g., the Rho family of small GTPases, p120cat, IQGAP, and PI3K) on cadherin dynamics and adhesion. The two applications of membrane microfluidics and micropatterns presented here significantly enhance the ability of such models to yield direct, relevant information about these interactions. Further applications of supported bilayer structuring, such as the creation of nanoscale and/or switchable barriers, will extend these ideas to capture additional aspects of membrane protein diffusion in experimental systems.

**Acknowledgment.** Studies in the laboratory of S.G.B. were supported by the NIH (GM069630) and by the NSF MRSEC Program (DMR-02-13618). Studies in the laboratory of W.J.N. were supported by the NIH (NS04275). L.K. was supported in part by the NIH NRSA (GM20878). T.D.P. was supported by a predoctoral fellowship from the HHMI. Additional support was provided by the Stanford Bio-X Interdisciplinary Initiatives Program. The Stanford Nanofabrication Facility is gratefully acknowledged for support in microfabrication.

LA052264A